



Radiative b -baryon decays to measure the photon and b -baryon polarization

Luis Miguel García Martín^{1,a}, Brij Jashal^{1,2,b}, Fernando Martínez Vidal^{1,c}, Arantza Oyanguren^{1,d}, Shibasis Roy^{3,4,e}, Ria Sain^{3,4,f}, Rahul Sinha^{3,4,g}

¹ IFIC, Universitat de València-CSIC, Apt. Correus 22085, 46071 València, Spain

² Tata Institute of Fundamental Research, Mumbai, India

³ The Institute of Mathematical Sciences, Taramani, Chennai 600113, India

⁴ Homi Bhabha National Institute Training School Complex, Anushakti Nagar, Mumbai 400085, India

Received: 12 April 2019 / Accepted: 8 July 2019 / Published online: 29 July 2019

© The Author(s) 2019

Abstract The radiative decays of b -baryons facilitate the direct measurement of photon helicity in $b \rightarrow s\gamma$ transitions thus serving as an important test of physics beyond the Standard Model. In this paper we analyze the complete angular distribution of ground state b -baryon radiative decays to multibody final states assuming an initially polarized b -baryon sample. Our sensitivity study suggests that the photon polarization asymmetry can be extracted to a good accuracy along with a simultaneous measurement of the initial b -baryon polarization. With higher yields of b -baryons, achievable in subsequent runs of the Large Hadron Collider (LHC), we find that the photon polarization measurement can play a pivotal role in constraining different new physics scenarios.

1 Introduction

The flavour-changing neutral current decays are known to be excellent probes of physics beyond the Standard Model (SM) [1–4]. Of particular interest are the loop level Glashow–Iliopoulos–Maiani (GIM) mechanism suppressed processes involving $b \rightarrow s\gamma$ transitions that enable the photon polarization to be measured. The helicity flip required for the dipole transition in such decays is sensitive to new physics (NP). Unfortunately, the helicity structure of the quark level $b \rightarrow s\gamma$ transition is hard to analyze using spinless B

mesons, as handedness of the quark is difficult to retrieve after hadronization [5–12].

Recently the LHCb experiment performed several indirect measurements concerning the photon polarization in the B and B_s meson systems. Polarized photons in $b \rightarrow s\gamma$ transitions were observed for the first time by analyzing the up-down asymmetry in $B^+ \rightarrow K^+ \pi^- \pi^+ \gamma$ decays [13]. Angular observables in the $B^0 \rightarrow K^{*0} e^+ e^-$ channel for dielectron invariant masses of less than 1 GeV/ c^2 , sensitive to the polarization of the virtual photon, were measured in [14]. The first experimental study of the photon polarization in radiative B_s^0 decays was reported in [15] by analyzing the time dependence of the $B_s^0 \rightarrow \phi\gamma$ decay rate.

A large number of b -baryons are also being produced at LHCb allowing for several interesting measurements to be performed using the ground state spin-1/2 b -baryons. The study of spin correlations in radiative decays of b -baryons allows one to directly infer the chirality of the dipole transition involved. The observable of interest, namely, the photon polarization asymmetry α_γ , defined as the ratio of shortfall in the observed number of right polarized photons compared to left polarized photons to the total number, is well recognized in the context of b -baryon radiative decays and has resulted in several studies [16–26]. Despite the rich phenomenology, the photon polarization asymmetry in radiative b -baryon decays is yet to be explored in experiments. In addition, it is worth mentioning that the initial b -baryon can have non-zero transverse polarization [27, 28] depending on the various production mechanism of a b -quark at the Large Hadron Collider (LHC). For finite quark masses ($m_b \neq 0$), a b -quark produced in a QCD process can have transverse polarization of the order of 10% [28, 29]. During hadronization, the polarization of the b -quark is retained to a large extent by the b -baryon as the depolarization effects [28] due to QCD interactions are

^a e-mail: Luis.Miguel.Garcia@ific.uv.es

^b e-mail: brij.kishor.jashal@cern.ch

^c e-mail: Fernando.Martinez@ific.uv.es

^d e-mail: Arantza.Oyanguren@ific.uv.es

^e e-mail: shibasisr@imsc.res.in

^f e-mail: riasain@imsc.res.in

^g e-mail: sinha@imsc.res.in

suppressed by a factor of Λ_{QCD}/m_b , a feature common to all b -baryons. A systematic study of b -baryon polarization P_b [30,31], defined as the production asymmetry between its up and down spin components, is therefore important for our understanding of the production mechanism and hadronization process of heavy quarks.

In this paper we revisit the $\Lambda_b^0 \rightarrow \Lambda^0 \gamma$ and the analogous $\Xi_b^- \rightarrow \Xi^- \gamma$ decays. The Λ^0 and Ξ^- subsequently decay to multibody final states that provide powerful handles not only on the photon polarization but also the initial b -baryon polarization. The complete angular distribution of the decay chains $\Lambda_b^0 \rightarrow \Lambda^0 \gamma$ and $\Xi_b^- \rightarrow \Xi^- (\rightarrow \Lambda^0 \pi^-) \gamma$, with the Λ^0 decaying into $p \pi^-$, is a function of the photon polarization, α_γ , the initial b -baryon polarization, P_b , and known decay asymmetry parameters of intermediate baryons. We explore the potential of simultaneous measurement of the photon and b -baryon polarizations at LHCb through the study of the angular distribution of b -baryon decays using Monte Carlo simulations. With the expected yield from the LHC Run II a sensitivity of about 0.15 is achievable for the photon polarization along with a measurement of Λ_b^0 polarization with a precision better than 10%. Despite of the challenges in Ξ_b^- due to scarcity of data, the decay mode $\Xi_b^- \rightarrow \Xi^- \gamma$ remains a promising channel for Run II and beyond where a sensitivity of the order of 0.2 can be achieved in α_γ measurement along with a first time measurement of Ξ_b polarization.

The paper is laid out as follows: in Sect. 2 we have discussed the angular distribution of the radiative decays [32,33] of Λ_b^0 and Ξ_b^- . Section 3 is devoted to the sensitivity analysis of these rare decays at the LHCb experiment. Finally, we provide constraints on new physics scenarios from the photon polarization asymmetry in Sect. 4 before concluding in Sect. 5.

2 Angular distribution of radiative b -baryon decays

2.1 Case study of $\Lambda_b^0 \rightarrow \Lambda^0 \gamma$

Assuming an initially polarized sample of Λ_b we study the complete angular distribution of $\Lambda_b^0 \rightarrow \Lambda^0 \gamma$ where the Λ subsequently decays to a proton (p) and pion (π^-). The transverse Λ_b^0 polarization is defined [30,31] as the mean value of the Λ_b^0 spin along the unit vector

$$\hat{n} = \frac{\vec{p}_p \times \vec{p}_{\Lambda_b}}{|\vec{p}_p \times \vec{p}_{\Lambda_b}|}, \tag{1}$$

normal to the production plane, where \vec{p}_p is the counter-clockwise proton beam direction and \vec{p}_{Λ_b} the Λ_b^0 momentum. A schematic view of the decay is shown in Fig. 1. The primary decay of $\Lambda_b^0 \rightarrow \Lambda^0 \gamma$ is described by two complex helicity amplitudes $H_{\lambda_\Lambda, \lambda_\gamma}$ with $\lambda_\Lambda = \pm 1/2, \lambda_\gamma = \pm 1$

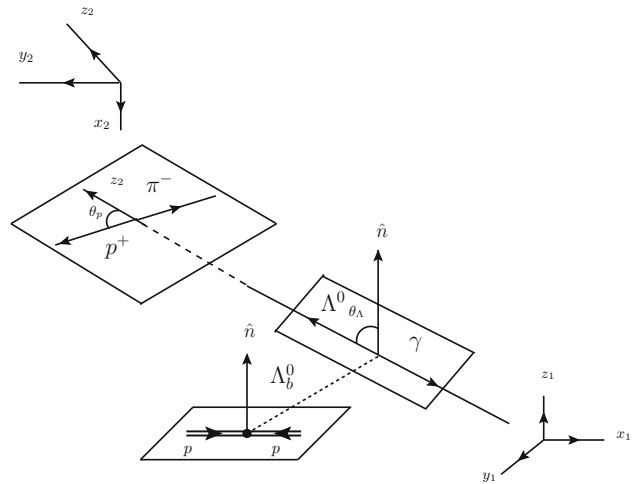


Fig. 1 Schematic view of the $\Lambda_b^0 \rightarrow \Lambda^0 \gamma$ decay

referring to the helicity values of the respective particles [34]. To define the angles we consider two Cartesian coordinate systems attached to the rest frames of Λ_b^0 and Λ^0 . In the rest frame of Λ_b^0 , the z_1 -axis is chosen to be parallel to the Λ_b^0 polarization direction \hat{n} . The relevant kinematic variables are defined as follows:

- θ_Λ is the polar angle of the Λ^0 momentum relative to \hat{n} in Λ_b^0 rest frame, $0 \leq \theta_\Lambda < \pi$.
- θ_p, ϕ_p are the polar and azimuthal angle of the proton momentum defined with respect to the axes $z_2 = \vec{p}_\Lambda / |\vec{p}_\Lambda|$ and $y_2 = \hat{n} \times \vec{p}_\Lambda / |\hat{n} \times \vec{p}_\Lambda|$ in Λ^0 rest frame.

The angular distribution is:

$$W(\theta_\Lambda, \theta_p) \propto 1 - \alpha_\Lambda P_{\Lambda_b} \cos \theta_p \cos \theta_\Lambda - \alpha_\gamma (\alpha_\Lambda \cos \theta_p - P_{\Lambda_b} \cos \theta_\Lambda) \tag{2}$$

Here, P_{Λ_b} is the initial Λ_b polarization and α_Λ is the Λ^0 weak decay parameter, defined in Table 1.

2.2 Case study of $\Xi_b^- \rightarrow \Xi^- \gamma$

Assuming an initially polarized sample of Ξ_b^- we study the complete angular distribution of $\Xi_b^- \rightarrow \Xi^- \gamma$, considering the subsequent decay $\Xi^- \rightarrow \Lambda^0 \pi^-$. The Λ^0 further decays to a proton and pion, resulting in a $p \pi^- \pi^- \gamma$ final state. The transverse polarization of Ξ_b^- is defined as the mean value of Ξ_b^- spin along the unit vector

$$\hat{n} = \frac{\vec{p}_p \times \vec{p}_{\Xi_b}}{|\vec{p}_p \times \vec{p}_{\Xi_b}|}, \tag{3}$$

normal to the production plane, where \vec{p}_p is the counter-clockwise proton beam direction and \vec{p}_{Ξ_b} the Ξ_b^- momen-

Table 1 Definition and measured values of the decay parameters and photon polarization used in Eqs. (2) and (4)

Expression	Obs. values	
α_γ	$\frac{ H_{\lambda_{\mathcal{E}}=-1/2, \lambda_\gamma=-1} ^2 - H_{\lambda_{\mathcal{E}}=1/2, \lambda_\gamma=1} ^2}{ H_{\lambda_{\mathcal{E}}=-1/2, \lambda_\gamma=-1} ^2 + H_{\lambda_{\mathcal{E}}=1/2, \lambda_\gamma=1} ^2}$	-
$\alpha_{\mathcal{E}}$	$\frac{ H_{\lambda_{\Lambda}=1/2} ^2 - H_{\lambda_{\Lambda}=-1/2} ^2}{ H_{\lambda_{\Lambda}=1/2} ^2 + H_{\lambda_{\Lambda}=-1/2} ^2}$	-0.458 ± 0.012 [35]
α_Λ	$\frac{ H_{\lambda_p=1/2} ^2 - H_{\lambda_p=-1/2} ^2}{ H_{\lambda_p=1/2} ^2 + H_{\lambda_p=-1/2} ^2}$	0.642 ± 0.013 [35]
$z_{\mathcal{E}}$	$\frac{H_{\lambda_{\Lambda}=1/2}^* H_{\lambda_{\Lambda}=-1/2}}{ H_{\lambda_{\Lambda}=1/2} ^2 + H_{\lambda_{\Lambda}=-1/2} ^2}$	-

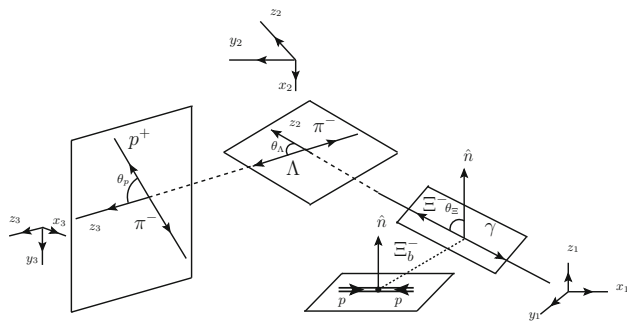


Fig. 2 Schematic view of the $\mathcal{E}_b^- \rightarrow \mathcal{E}^- \gamma$ decay

tum. A schematic view of the decay is shown in Fig. 2. The primary decay $\mathcal{E}_b^- \rightarrow \mathcal{E}^- \gamma$ is described by two complex helicity amplitudes $H_{\lambda_{\mathcal{E}}, \lambda_\gamma}$ with $\lambda_{\mathcal{E}} = \pm 1/2$, $\lambda_\gamma = \pm 1$ referring to the helicity values of the respective particles. To define the angles we consider three Cartesian coordinate systems attached to the rest frames of \mathcal{E}_b^- , \mathcal{E}^- and Λ^0 . In the rest frame of \mathcal{E}_b^- , the z_1 -axis is chosen to be parallel to the \mathcal{E}_b^- polarization direction \hat{n} . Similar to the previous case, the relevant kinematic variables are defined as follows:

- $\theta_{\mathcal{E}}$ is the polar angle of the \mathcal{E}^- momentum relative to \hat{n} in \mathcal{E}_b^- rest frame, $0 \leq \theta_{\mathcal{E}} < \pi$.
- $\theta_\Lambda, \phi_\Lambda$ are the polar and azimuthal angle of the Λ^0 momentum defined with respect to the axes $z_2 = \vec{p}_{\mathcal{E}} / |\vec{p}_{\mathcal{E}}|$ and $y_2 = \hat{n} \times \vec{p}_{\mathcal{E}} / |\hat{n} \times \vec{p}_{\mathcal{E}}|$ in \mathcal{E} rest frame.
- θ_p, ϕ_p are the polar and azimuthal angle of the proton momentum defined with respect to the axes $z_3 = \vec{p}_\Lambda / |\vec{p}_\Lambda|$ and $y_3 = \hat{n} \times \vec{p}_\Lambda / |\hat{n} \times \vec{p}_\Lambda|$ in Λ^0 rest frame.

The complete angular distribution reads,

$$W(\eta, \theta_\Lambda, \theta_p, \theta_{\mathcal{E}}) \propto 1 + \alpha_\Lambda \alpha_{\mathcal{E}} \cos \theta_p + \alpha_\gamma \alpha_{\mathcal{E}} \cos \theta_\Lambda + \alpha_\Lambda \alpha_\gamma \cos \theta_p \cos \theta_\Lambda - 2\alpha_\Lambda \alpha_\gamma \text{Re}(e^{i\eta} z_{\mathcal{E}}) \sin \theta_p \sin \theta_\Lambda - P_{\mathcal{E}_b} \alpha_{\mathcal{E}} \cos \theta_{\mathcal{E}} \cos \theta_\Lambda - P_{\mathcal{E}_b} \alpha_\gamma \cos \theta_{\mathcal{E}} \quad (4)$$

$$- P_{\mathcal{E}_b} \alpha_{\mathcal{E}} \alpha_\Lambda \alpha_\gamma \cos \theta_{\mathcal{E}} \cos \theta_p - P_{\mathcal{E}_b} \alpha_\Lambda \cos \theta_{\mathcal{E}} \cos \theta_\Lambda \cos \theta_p + 2\alpha_\Lambda P_{\mathcal{E}_b} \text{Re}(e^{i\eta} z_{\mathcal{E}}) \cos \theta_{\mathcal{E}} \sin \theta_p \sin \theta_\Lambda,$$

where $\eta = \phi_\Lambda - \phi_p$, and the \mathcal{E}_b^- polarization matrix $\rho_{\lambda_{\mathcal{E}_b}, \lambda'_{\mathcal{E}_b}}$ is defined as $\rho_{\frac{1}{2}, \frac{1}{2}} + \rho_{-\frac{1}{2}, -\frac{1}{2}} = 1$ and $\text{Tr}[\rho \hat{n}] = (\rho_{\frac{1}{2}, \frac{1}{2}} - \rho_{-\frac{1}{2}, -\frac{1}{2}}) \hat{z} = P_{\mathcal{E}_b} \hat{z}$, with the off-diagonal entries averaging out to zero in absence of correlation between production and decay mechanisms. Here $P_{\mathcal{E}_b}$ is the initial \mathcal{E}_b^- polarization, and $\alpha_{\mathcal{E}}$ is the \mathcal{E}^- weak decay parameter. The complete expressions of decay parameters and their values are summarized in Table 1.

3 Experimental prospects at the LHCb experiment

The potential to measure the photon and b -baryon polarization at LHCb through the angular distribution of b -baryon decays can be studied using fast Monte Carlo simulation method. The expected sensitivity as a function of the values of the α_γ , P_{Λ_b} and $P_{\mathcal{E}_b}$ parameters, and depending on the number of reconstructed events, is determined. Effects due to the angular acceptance and resolution, coming from the event reconstruction, are included in the simulations. The impact of the amount and shape of the possible background is also studied. Results are detailed along this section. Since the expected number of events depend on the b -hadron production fractions in proton-proton collisions at the LHC energy, a summary of the present status is discussed below.

3.1 b -baryon fragmentation fractions

There are various processes through which a b quark can be produced in LHC. The b quark can then combine with a light diquark to produce a b -baryon. The probability of a b -quark fragment into a baryon is given by the fragmentation fraction (f_B). It is customary to express the fragmentation fraction [29, 36–38] for a specific b -baryon as

$$R_B = \frac{f_B}{f_i + f_j}, \quad (5)$$

where (f_i, f_j) are: (f_u, f_d) for $B = \Lambda_b^0$, (f_u, f_s) for $B = \mathcal{E}_b^0$, (f_d, f_s) for $B = \mathcal{E}_b^-$ and $f_{u,d,s} \equiv \mathcal{B}(b \rightarrow B^-, \bar{B}^0, \bar{B}_s^0)$. R_B is experimentally measured [39, 40] and along with the knowledge of $f_{u,s,d}$ one can estimate f_B [36, 41, 42]. It is important to note that $f_{\Lambda_b} / (f_u + f_d)$ has a dependence on p_T of the final state particles [36, 39, 43]. Latest results from LHCb yields [39]

$$\frac{f_{\Lambda_b}}{f_u + f_d} = 0.404 \pm 0.017 \pm 0.027 \pm 0.105. \quad (6)$$

Recently LHCb has measured the fragmentation fraction of a b quark hadronizing into a \mathcal{E}_b^- ($f_{\mathcal{E}_b^-}$) with respect to

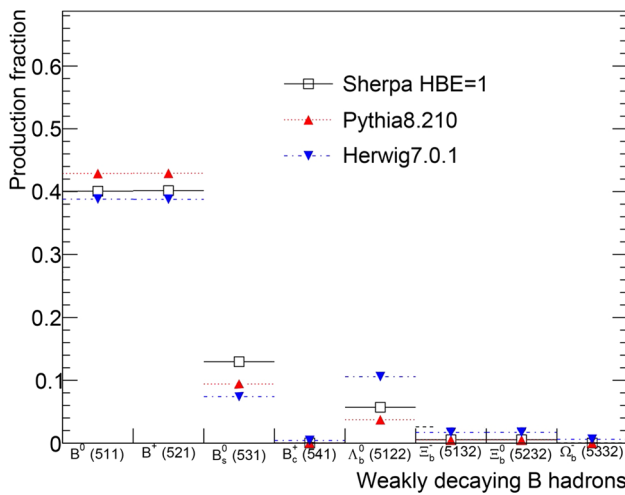


Fig. 3 *b*-hadron production fractions at LHC extracted from several physics generators: Sherpa [47], Pythia [48] and Herdwig [49]. In the case of Sherpa HBE = 1 the Heavy Baryon Enhancement parameter (HBE) is set to one to improve the modelling of heavy quark hadronization

fragmentation fraction of a *b* quark hadronizing into a Λ_b (f_{Λ_b}), using the $\Xi_b^- \rightarrow \Xi^- J/\psi$ and $\Lambda_b \rightarrow \Lambda J/\psi$ decay modes [44–46].

Using the data samples collected at $\sqrt{s} = 7, 8,$ and 13 TeV to measure the ratio of production rates of Ξ_b^- to Λ_b^0 , with pseudorapidity and p_T in the range $2 \leq \eta \leq 6, p_T \leq 20 \text{ GeV}/c$, LHCb measured the following values:

$$\begin{aligned} \frac{f_{\Xi_b^-}}{f_{\Lambda_b}} &= (6.7 \pm 2.1) \times 10^{-2} \quad [\sqrt{s} = 7 \text{ and } 8 \text{ TeV}], \\ \frac{f_{\Xi_b^-}}{f_{\Lambda_b}} &= (8.2 \pm 2.6) \times 10^{-2} \quad [\sqrt{s} = 13 \text{ TeV}]. \end{aligned} \quad (7)$$

In these results the uncertainty is dominated by the departure from the SU(3) relation $\Gamma(\Xi_b^- \rightarrow \Xi^- J/\psi) = \frac{2}{3} \Gamma(\Lambda_b^0 \rightarrow \Lambda^0 J/\psi)$, coming from SU(3) breaking of the order of 30% [44].

The fraction of *b*-baryon species produced in proton proton collisions at $\sqrt{s}=1.96$ TeV is about 22% [35]. Assuming that this proportion remains constant at $\sqrt{s} = 13$ TeV, and that the total cross section $\sigma(\text{pp} \rightarrow b\bar{b}X)$ is $\approx 600 \mu\text{b}$ [42], we get the values $\sigma(\text{pp} \rightarrow \Lambda_b)^{13\text{TeV}} \sim 117 \mu\text{b}$ and $\sigma(\text{pp} \rightarrow \Xi_b)^{13\text{TeV}} \sim 12 \mu\text{b}$. In this estimation the Ω_b^- contribution is taken to be about 10% of the Ξ_b^- . These values are inside the range of the predictions by several Monte Carlo generators, as shown in Fig. 3.

3.2 Fit procedure

An unbinned maximum likelihood fit is used to determine the photon and *b*-baryon polarization. The angular distribution for Λ_b^0 in Sect. 2.1 allows to extract the photon polarization

fixing the Λ_b^0 polarization, or extracting both parameters at the same time. Thus, Eq. (2) is used for obtaining these two polarizations simultaneously. The dependence on the initial *b*-baryon polarization can be eliminated by integrating out the $\cos\theta_\Lambda$ in Eq. (2) obtaining:

$$W(\theta_p) \propto 1 - \alpha_\gamma \alpha_\Lambda \cos\theta_p. \quad (8)$$

In the case of Ξ_b^- angular distribution of Sect. 2.2, it is possible to integrate out the azimuthal angle η in Eq. (4). This removes the dependence on the unknown z_Ξ parameter:

$$\begin{aligned} W(\theta_\Lambda, \theta_p, \theta_\Xi) &\propto 1 + \alpha_\Lambda \alpha_\Xi \cos\theta_p + \alpha_\gamma \alpha_\Xi \cos\theta_\Lambda \\ &+ \alpha_\Lambda \alpha_\gamma \cos\theta_p \cos\theta_\Lambda - P_{\Xi_b} \alpha_\Xi \cos\theta_\Xi \cos\theta_\Lambda \\ &- P_{\Xi_b} \alpha_\gamma \cos\theta_\Xi - P_{\Xi_b} \alpha_\Xi \alpha_\Lambda \alpha_\gamma \cos\theta_\Xi \cos\theta_p \\ &- P_{\Xi_b} \alpha_\Lambda \cos\theta_\Xi \cos\theta_\Lambda \cos\theta_p. \end{aligned} \quad (9)$$

This expression is used in the fit to extract the photon and Ξ_b^- polarization simultaneously. Integrating out the $\cos\theta_\Xi$ angle in Eq. (9), the dependence with the *b*-baryon polarization can also be removed:

$$\begin{aligned} W(\theta_\Lambda, \theta_p) &\propto 1 + \alpha_\Lambda \alpha_\Xi \cos\theta_p + \alpha_\gamma \alpha_\Xi \cos\theta_\Lambda \\ &+ \alpha_\Lambda \alpha_\gamma \cos\theta_p \cos\theta_\Lambda. \end{aligned} \quad (10)$$

In order to validate the fit procedure, to check consistency between pseudo-experiments and to detect possible biases in the distribution of the fitted parameters, pull distributions, defined as the difference between the fitted and generated values, divided by the uncertainty from the fit, are determined. It is found that there is no bias in the fit and the pull distributions are correct.

3.3 Measurement of $\alpha_\gamma, P_{\Lambda_b}$ and P_{Ξ_b}

To understand the correlation of the value of the α_γ parameter and its uncertainty, a large number of pseudo-experiments of 1000 events each are generated according to Eqs. (2) and (4) for the Λ_b^0 and Ξ_b^- decay channels respectively. The generated value of α_γ is varied in this study between -1.0 and $+1.0$ and the angular distribution is fitted for each case. The results of the fits are shown in Fig. 4a. A small dependence with the value of the photon polarization is observed for both channels, with maximum sensitivity at larger slopes, $+1$ and -1 values of the α_γ parameter. The sensitivity for the $\Lambda_b^0 \rightarrow \Lambda^0 \gamma$ decay channel is found to be slightly better (about 15%) as compared to the $\Xi_b^- \rightarrow \Xi^- \gamma$ channel. This is coming from the larger absolute value of the weak decay parameter, α_Λ , compared to the α_Ξ parameter (see Eqs. (8) and (10)). Figure 4b shows the expected sensitivity to the α_γ parameter as function of the reconstructed number of events for both channels. Pseudo-experiments with samples ranging

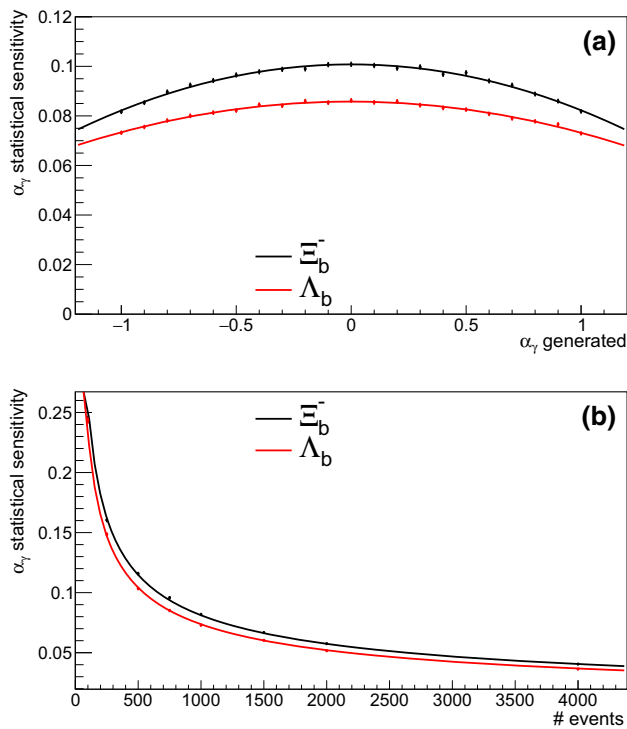


Fig. 4 **a** Sensitivity to the photon polarization parameter as function of its value for the Λ_b^0 and Ξ_b^- decay channels. Dots with errors correspond to the fit results. A second order polynomial is superimposed for better visualization. **b** Statistical sensitivity of the photon polarization as function of the reconstructed number of events for the Λ_b^0 and Ξ_b^- cases. In this case was fitted to a function $1/\sqrt{x}$

Table 2 Expected signal yield for $\Lambda_b^0 \rightarrow \Lambda^0 \gamma$ and $\Xi_b^- \rightarrow \Xi^- \gamma$ decay channels

	$\Lambda_b^0 \rightarrow \Lambda^0 \gamma$	$\Xi_b^- \rightarrow \Xi^- \gamma$
$\sigma(\text{pp} \rightarrow H_b) 13\text{TeV} (\mu\text{b})$	117	12
$BR(H_b \rightarrow H\gamma)$	10^{-5}	10^{-5}
$BR(\Xi^- \rightarrow \Lambda^0 \pi^-)$	–	1.0
$BR(\Lambda^0 \rightarrow p^+ \pi^-)$	0.64	0.64
$\epsilon_{H_b \rightarrow H\gamma}$	1.0×10^{-4}	1.0×10^{-4}
N (Run II, 6fb^{-1})	900	92
N (Run III, 25fb^{-1})	3740	384

between 100 and 4000 events are generated in this study with the Standard Model expectation of $\alpha_\gamma = 1$. The results show that the photon polarization can be potentially measured with less than 10% uncertainty with the reconstruction of about 1000 radiative b -baryon events.

In Table 2 the expected number of events for the different run periods at LHCb are estimated. Numbers are obtained according to the production fractions of the different b -baryon species (see Sect. 3.1) and assuming that the branching fraction for radiative b -baryon decays is about 10^{-5} [50], in agreement with recent [51] LHCb results. A reconstruc-

tion efficiency of order 10^{-4} is considered. This estimation is obtained by scaling the reconstruction efficiency for radiative B meson decays in [15] by a factor of 1/100. This assumption takes into account that the trigger and reconstruction algorithms at LHCb are less efficient for long living particles [52]. Besides, one expects the need of tighter selection criteria to suppress the large amount of combinatorial background expected from prompt Λ^0 's and random photons.

Since the angular distribution of radiative b -baryon decays is also sensitive to the initial b -baryon polarization (see Eqs. (2) and (9)), one can extract P_{Λ_b} and P_{Ξ_b} values together with the photon polarization. Pseudo-experiments with 1000 events each are performed in this study using several values of the Λ_b^0 and Ξ_b^- polarization, fitting simultaneously α_γ and P_{Λ_b} , for the $\Lambda_b^0 \rightarrow \Lambda^0 \gamma$ decay channel, and α_γ and P_{Ξ_b} for the $\Xi_b^- \rightarrow \Xi^- \gamma$ decay channel. Since the P_{Ξ_b} in hadron collisions is expected to be similar to the polarization of the Λ_b , which has been measured in [53], a maximum polarization of 10% for the initial b -baryon polarization is considered in the generation for both channels. The results of the achieved sensitivity for the α_γ and P_{Λ_b} or P_{Ξ_b} parameters as a function of its value is shown in Fig. 5.

As it can be seen in Fig. 5b, the sensitivity to the α_γ parameter is not affected by the measurement of the Ξ_b^- polarization in the simultaneous fit, given enough statistics. This is also true for the same study with the Λ_b^0 polarization. In addition, the value of the Λ_b^0 and Ξ_b^- polarization parameters can be extracted with good accuracy independently of its value, with improved precision as the photon polarization approaches the SM value.

3.4 Event reconstruction and background effects

To include the effect of the signal event reconstruction and background sources the angular distribution in Eqs. (8) and (10) is modified. The signal probability density distribution is affected by an angular acceptance, $\mathcal{A}(\theta_\Lambda, \theta_p)$, and a resolution function, $\mathcal{R}(\theta_\Lambda, \theta_p; \theta'_\Lambda, \theta'_p)$. Additionally, background sources with different angular shapes f_B and signal to background rate (S/B) are also considered in the fitting procedure. The angular distributions of the Λ_b^0 and Ξ_b^- decay channels are modified:

$$\Gamma(\theta'_\Lambda, \theta'_p; \alpha_\gamma) = \left(f_S(\theta_\Lambda, \theta_p; \alpha_\gamma) \times \mathcal{A}(\theta_\Lambda, \theta_p) \right) * \mathcal{R}(\theta_\Lambda, \theta_p; \theta'_\Lambda, \theta'_p) + \frac{S}{B} (f_B(\theta_\Lambda, \theta_p))$$

The LHCb detector has been described elsewhere [54,55]. The resolution of the proton and Λ^0 polar angles are expected to be worse if the Λ^0 particle decays after the first LHCb tracker, since the vertex and momentum resolutions degrade. If the information of the LHCb VELO detector is not included in the reconstruction of the proton and pion candidates,

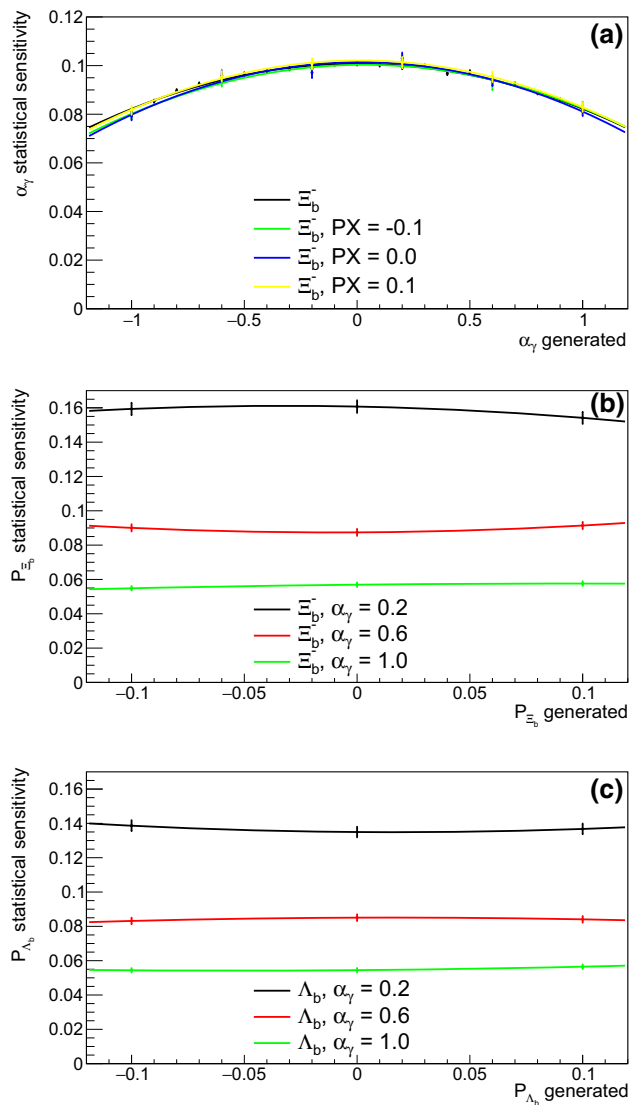


Fig. 5 **a** Sensitivity to the photon polarization as function of its value for different assumptions of the initial Ξ_b^- polarization. The black line corresponds to the fit of Eq. (10), which does not include the polar angle of the Ξ^- momentum relative to the normal vector to the production plane, while the other line correspond to the fit of Eq. (9). Similar results are obtained for the Λ_b^0 polarization. **b** Sensitivity to the Ξ_b^- polarization as function of its value for Ξ_b^- for different values of α_γ using Eq. (9). **c** Sensitivity to the Λ_b^0 polarization as function of its value for Λ_b^0 for different values of α_γ using Eq. (9). In these figures dots with errors correspond to the fit results. A second order polynomial is superimposed for better visualization

named *downstream* track category, the angular resolution can be as large as 90 mrad [56]. Since Λ^0 particles have a long lifetime, most of the events are expected in this category. No bias in the mean of the angular resolution is expected. For tracks which are reconstructed including the information of the VELO detector, named *long* track category, the angular resolution is expected to be better. Monte Carlo simulations are performed using angular resolutions from 30 to 90 mrad.

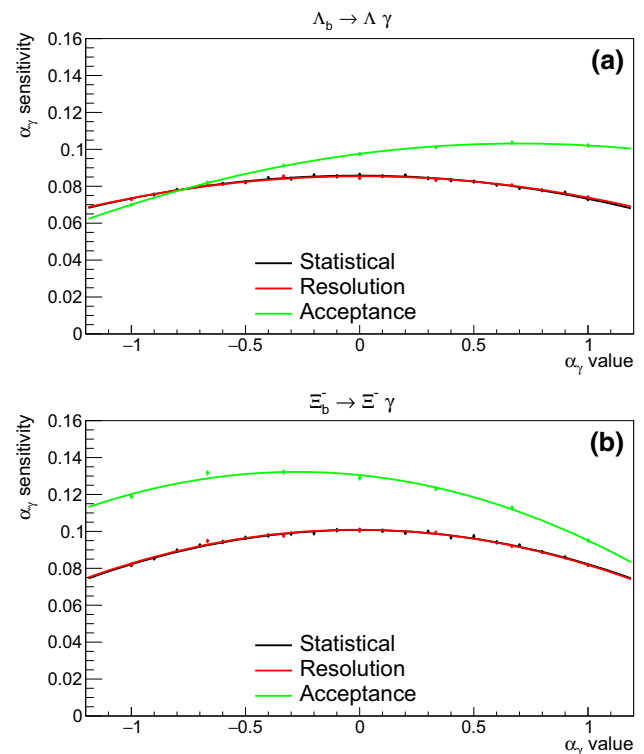


Fig. 6 **a** Sensitivity to the photon polarization as function of its value for Λ_b^0 (a) and Ξ_b^- (b) cases including angular resolution and acceptance effects. Dots with errors corresponds to the fit results. A second order polynomial is superimposed for better visualization

Since the angular distributions are quite smooth the resolution is expected to have a negligible effect. Figure 6 shows the effect of the resolution and angular acceptance for the Λ_b^0 and Ξ_b^- cases.

The angular acceptance is expected to be due to trigger and reconstruction selection criteria. The dominant source of bias is expected to come from pion momentum requirements, affecting the proton and Λ^0 angles in an asymmetric way. Following the results obtained in [30] for the proton angle, a third order polynomial function is implemented for the acceptance. Pseudo-experiments are generated using this function. Results of the fits, including the acceptance, are shown in Fig. 6. An important effect on the sensitivity to the photon polarization is observed, which will have to be controlled using data control samples. For the case of the Ξ_b^- small correlation between the proton and Λ^0 angles is expected.

One of the most important challenges when reconstructing radiative b -baryon decays is expected to be the background suppression. Since strange b -baryons have large lifetimes, and photons are involved in the decays, making a vertex fit from the b -baryon decay products is not possible. A large amount of combinatorial background is then expected from random photons and prompt Λ^0 particles. In this study

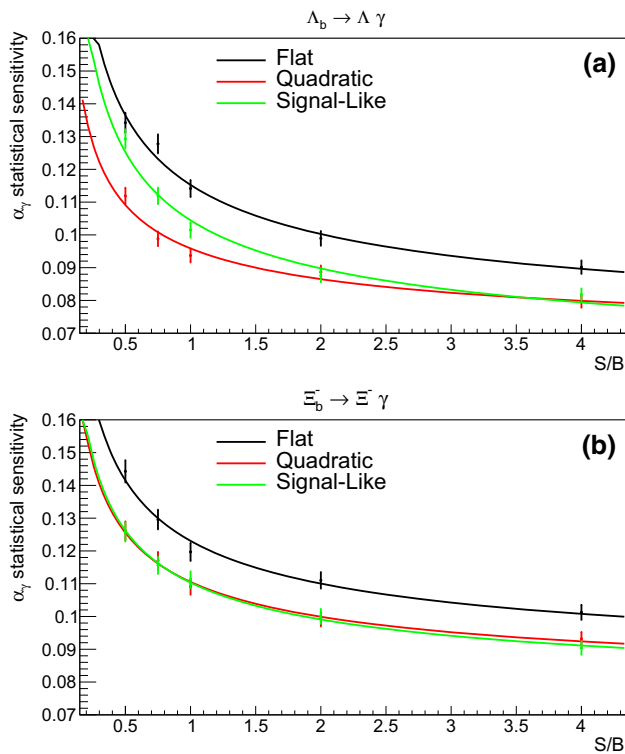


Fig. 7 Sensitivity to the photon polarization as function of the signal over background ratio for Λ_b^0 (a) and Ξ_b^- (b) including background effects. Dots with errors corresponds to the fit results. A function $A + B/\sqrt{x}$ is superimposed for better visualization

a background source is considered and a large number of pseudo-experiments is generated and fitted considering different signal (S) to background (B) rates, as well as different shapes for the angular distribution of the background. The signal samples are of 1000 events each, and the amount of events in the background sample are varied. A flat, signal-like and a second order polynomial are tested for the angular distribution of the background. The samples are generated with SM values of the photon polarization parameter, $\alpha_\gamma = 1$. Fig. 7 shows the results of the fit of the pseudo-experiments.

As it can be observed, the shape of the background is not so relevant as the background rejection capability. An important S/B rate is necessary in order to measure the photon polarization with an accuracy below 10%. To achieve this, multivariate analysis techniques will be crucial, in particular for rejecting the large amount of the expected combinatorial background.

3.5 Discussion of results

Assuming that the LHCb detector can reconstruct about 900 $\Lambda_b^0 \rightarrow \Lambda^0 \gamma$ events with the data of the Run II, and that systematic uncertainties can be controlled to the same order

of the statistical uncertainty, a sensitivity of about 0.15 could be achieved for the photon polarization parameter α_γ . The Λ_b^0 polarization can also be measured with a precision better than 10%, the sensitivity depending on the value of the photon polarization.

The measurement for the $\Xi_b^- \rightarrow \Xi^- \gamma$ decay channel is more challenging and will need more data to reach the same sensitivity but it is a promising channel for Run III and beyond. It has the advantage of an additional track coming from the $\Xi^- (\rightarrow \Lambda^0 \pi^-)$ and the possibility to reconstruct the charged Ξ^- baryon. If systematic uncertainties are controlled at the order of the statistical uncertainty, a sensitivity of around 0.2 could be achieved. This channel also offers the possibility to measure the Ξ_b^- polarization, which is unknown at present. The experimental angular resolution is found to have a negligible effect on the measurement of the photon polarization. In contrast, the effect of the angular acceptance due to the event reconstruction is found to be important and needs to be controlled from data.

The crucial task in these analyses is expected to be the background suppression. A signal-to-background rate less than one is needed to obtain a good precision in the photon polarization.

Estimations in Table 2 for the LHCb Run III do not assume any improvement of the LHCb detector, which is far from reality. In the next LHC run, from 2020-2023, in addition to upgrade its tracking and vertexing systems, the LHCb experiment will exploit a novel trigger concept where all sub-detectors are read out in real time and the first level trigger is fully software implemented. Track momenta resolution will improve by 10–20% [57,58]. For long living particles such as strange baryons, the efficiency is expected to increase at least by 10% using dedicated reconstruction algorithms [52], and could still be much larger with the improvement of the software trigger.

3.6 Normalization channel

A data-driven measurement of radiative b-baryon decays require the use of control and normalization decay modes. The $\Lambda_b^0 \rightarrow \Lambda^0 J/\psi (\rightarrow \mu^+ \mu^-)$ and $\Xi_b^- \rightarrow \Xi^- J/\psi (\rightarrow \mu^+ \mu^-)$ are chosen as the preferred modes of normalization for the $\Lambda_b^0 \rightarrow \Lambda^0 \gamma$ and $\Xi_b^- \rightarrow \Xi^- \gamma$ channels, respectively. The advantage of this choice is that most of the systematic uncertainties coming from the track reconstruction of b-baryons cancel when the ratio of rates are considered. Also the fragmentation fractions, which have at present large uncertainties (see Sect. 3.1), cancel. The relative number of events of the radiative and di-muonic channels is then:

$$\frac{N_{\Lambda_b^0 \rightarrow \Lambda^0 \gamma}}{N_{\Lambda_b^0 \rightarrow \Lambda^0 J/\psi}} = \frac{\mathcal{B}(\Lambda_b^0 \rightarrow \Lambda^0 \gamma) \epsilon_{\Lambda^0 \gamma}}{\mathcal{B}(\Lambda_b^0 \rightarrow \Lambda^0 J/\psi) \mathcal{B}(J/\psi \rightarrow \mu^+ \mu^-) \epsilon_{\Lambda^0 J/\psi}},$$

assuming the same luminosity for both channels, and taking into account that f_{Λ_b} , and $\mathcal{B}(\Lambda^0 \rightarrow p \pi^-)$ cancel in this ratio. $\epsilon_{\Lambda^0 \gamma}$ and $\epsilon_{\Lambda^0 J/\psi}$ are the remaining efficiencies which are different for both channels, coming mainly from photon and muon reconstruction. In a similar way:

$$\frac{N_{\Xi_b^- \rightarrow \Xi^- \gamma}}{N_{\Xi_b^- \rightarrow \Xi^- J/\psi}} = \frac{\mathcal{B}(\Xi_b^- \rightarrow \Xi^- \gamma) \epsilon_{\Xi^- \gamma}}{\mathcal{B}(\Xi_b^- \rightarrow \Xi^- J/\psi) \mathcal{B}(J/\psi \rightarrow \mu^+ \mu^-) \epsilon_{\Xi^- J/\psi}},$$

where again same luminosity for both channels is assumed, and f_{Ξ_b} , $\mathcal{B}(\Xi^- \rightarrow \Lambda^0 \pi^-)$ and $\mathcal{B}(\Lambda^0 \rightarrow p \pi^-)$ cancel. $\epsilon_{\Xi^- \gamma}$ and $\epsilon_{\Xi^- J/\psi}$ are the remaining efficiencies which are different for both channels. Note that no attempt is made to measure the angular distribution of di-muonic channels.

An alternative decay channel for normalization is the $B^0 \rightarrow K^{*0} \gamma$, which has larger efficiency but is also affected by larger amount of background. In this case the systematic uncertainty due to the photon reconstruction cancels.

4 New physics constraints

The process $b \rightarrow s \gamma$, at the leading order in α_s , gets contribution from dimension six electromagnetic dipole operators:

$$O_7^{(j)} = (em_b)/(16\pi^2) \bar{s} \sigma^{\alpha\beta} P_{R(L)} b F_{\alpha\beta}$$

corresponding to the emission of a left (L) or right (R) handed photon respectively. The small s -quark mass has been ignored in $O_7^{(j)}$ and $P_{R,L}$ are defined as $P_{R,L} = (1 \pm \gamma_5)/2$. The Hamiltonian corresponding to the decay is given by

$$\mathcal{H}_{eff} = \frac{-4G_F V_{tb} V_{ts}^*}{\sqrt{2}} (C_7 O_7 + C_7' O_7'), \tag{11}$$

where $C_7^{(j)}$ are the Wilson coefficients [17] describing the short distance contributions, V_{tb} and V_{ts} are the relevant Cabibbo–Kobayashi–Maskawa (CKM) matrix elements for the transition, and G_F is the Fermi constant. The polarization asymmetry α_γ in Table 1 can be thus defined as

$$\alpha_\gamma = \frac{\Gamma(\lambda_\gamma = L) - \Gamma(\lambda_\gamma = R)}{\Gamma(\lambda_\gamma = L) + \Gamma(\lambda_\gamma = R)}, \tag{12}$$

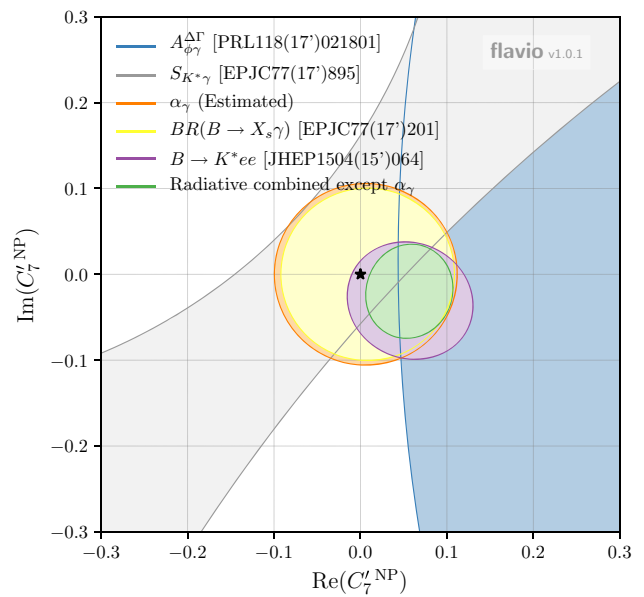


Fig. 8 New Physics constraints on $\text{Re}(C_7') - \text{Im}(C_7')$ using flavio [59, 60]. $A_{\phi\gamma}^{\Delta\Gamma}$ in blue, $S_{K^*\gamma}$ in violet, α_γ (assuming a value of $\alpha_\gamma = 1.0 \pm 0.15$) in orange, the inclusive radiative branching ratio in yellow, the angular study of $B \rightarrow K^* e^+ e^-$ in purple and the combination of all this measurement except for the α_γ one in green. Besides, the SM value is marked with a star

Within SM the contribution to right-handed photons is suppressed by the ratio $r = \frac{C_7'}{C_7} \simeq \frac{m_s}{m_b}$, resulting in

$$\alpha_\gamma = \frac{1 - |r|^2}{1 + |r|^2} \simeq 1. \tag{13}$$

However, various new physics (NP) scenarios as well as long distance effects within the SM can result in new contributions to the C_7' causing a departure from the SM value [59]. Long distance contribution has been estimated to be small and of the order of 5% [17]. Thus, any significant deviation of the measured value of α_γ from unity could indicate the presence of NP contributions to the Wilson coefficient C_7' . In general C_7' can have both real and imaginary contributions. There are, however, already constraints on C_7' using other measurements like A_{CP} , the direct CP asymmetry, S , the mixing-induced CP asymmetry and $A_{\Delta\Gamma}$, the mass-eigenstate rate asymmetry from the decays of neutral B_d and B_s mesons to CP eigenstates, for example in $B_s \rightarrow \phi \gamma$ or $B^0 \rightarrow K^*(\rightarrow K_S \pi^0) \gamma$ decays. In Fig. 8, the constraints in the C_7' plane from measurements of $A_{\Delta\Gamma}(B_s \rightarrow \phi \gamma)$, the inclusive branching ratio $Br(B \rightarrow X_s \gamma)$, $S(B \rightarrow K^* \gamma)$ and angular asymmetries of $B \rightarrow K^* e^+ e^-$ are shown. The constraint for an estimate of $\alpha_\gamma = 1.0 \pm 0.15$ is also plotted. With the expected sensitivity of α_γ it is clear that this measurement provides competitive constraints on new physics in comparison to the existing measurements using B mesons.

5 Conclusions

The flavour-changing GIM suppressed processes involving $b \rightarrow s\gamma$ transitions are known to be excellent probes of physics beyond the Standard Model. In that context, we analyze the decays $\Lambda_b^0 \rightarrow \Lambda^0 \gamma$ and $\Xi_b^- \rightarrow \Xi^- \gamma$ undergoing the same transition. By exploiting the spin correlations in radiative decays of b -baryons we demonstrate that they offer a convenient method for direct measurement of the photon polarization asymmetry α_γ along with a measurement of the initial b -baryon polarization. We presented expressions for the complete angular distribution of the decay chains $\Lambda_b^0 \rightarrow \Lambda^0 \gamma$ and $\Xi_b^- \rightarrow \Xi^- (\rightarrow \Lambda^0 \pi^-) \gamma$, with the Λ^0 decaying into $p \pi^-$, expressed as a function of α_γ , the photon polarization, P_b , the initial b -baryon polarization and known decay asymmetry parameters of intermediate baryons. We then explored the potential of joint measurement of the photon and b -baryon polarization at LHCb through the angular distribution study of b -baryon decays using Monte Carlo simulations. We find that with the expected yield from the LHC Run II a sensitivity of about 0.15 is achievable for the photon polarization along with a measurement of Λ_b^0 polarization with a precision better than 10%. Despite of the challenges in Ξ_b^- due to scarcity of data, even Run II allows a sensitivity of the order of 0.2 to be achieved for α_γ along with a first time measurement of $P_{\Xi_b^-}$. With higher yields, achievable in subsequent runs of the Large Hadron Collider, the photon polarization measurement using b -baryons will play a pivotal role in constraining different new physics scenarios.

Acknowledgements We thank L. Oliver for the interesting and motivating discussions at the beginning of this work. Part of this work is supported by the Spanish Ministerio of Economía, Industria and Competitividad.

Data Availability Statement This manuscript has no associated data or the data will not be deposited. [Authors' comment: The data is simulated using fast Monte Carlo simulation. Not applicable.]

Open Access This article is distributed under the terms of the Creative Commons Attribution 4.0 International License (<http://creativecommons.org/licenses/by/4.0/>), which permits unrestricted use, distribution, and reproduction in any medium, provided you give appropriate credit to the original author(s) and the source, provide a link to the Creative Commons license, and indicate if changes were made. Funded by SCOAP³.

References

- M. Misiak, Nucl. Phys. B **393**, 23 (1993) Erratum: [Nucl. Phys. B **439**, 461 (1995)]. [https://doi.org/10.1016/0550-3213\(95\)00029-R](https://doi.org/10.1016/0550-3213(95)00029-R). [https://doi.org/10.1016/0550-3213\(93\)90235-H](https://doi.org/10.1016/0550-3213(93)90235-H)
- A.J. Buras, M. Misiak, M. Munz, S. Pokorski, Nucl. Phys. B **424**, 374 (1994). [https://doi.org/10.1016/0550-3213\(94\)90299-2](https://doi.org/10.1016/0550-3213(94)90299-2). [arXiv:hep-ph/9311345](https://arxiv.org/abs/hep-ph/9311345)
- K.G. Chetyrkin, M. Misiak, M. Munz, Phys. Lett. B **400**, 206 (1997) Erratum: [Phys. Lett. B **425**, 414 (1998)]. [https://doi.org/10.1016/S0370-2693\(97\)00324-9](https://doi.org/10.1016/S0370-2693(97)00324-9). [arXiv:hep-ph/9612313](https://arxiv.org/abs/hep-ph/9612313)
- F. Kruger, L.M. Sehgal, N. Sinha, R. Sinha, Phys. Rev. D **61**, 114028 (2000) Erratum: [Phys. Rev. D **63**, 019901 (2001)]. <https://doi.org/10.1103/PhysRevD.61.114028>. <https://doi.org/10.1103/PhysRevD.63.019901>. [arXiv:hep-ph/9907386](https://arxiv.org/abs/hep-ph/9907386)
- Y. Grossman, D. Pirjol, JHEP **0006**, 029 (2000). <https://doi.org/10.1088/1126-6708/2000/06/029>. [arXiv:hep-ph/0005069](https://arxiv.org/abs/hep-ph/0005069)
- M. Gronau, Y. Grossman, D. Pirjol, A. Ryd, Phys. Rev. Lett. **88**, 051802 (2002). <https://doi.org/10.1103/PhysRevLett.88.051802>. [arXiv:hep-ph/0107254](https://arxiv.org/abs/hep-ph/0107254)
- M. Gronau, D. Pirjol, Phys. Rev. D **66**, 054008 (2002). <https://doi.org/10.1103/PhysRevD.66.054008>. [arXiv:hep-ph/0205065](https://arxiv.org/abs/hep-ph/0205065)
- T. Hurth, Rev. Mod. Phys. **75**, 1159 (2003). <https://doi.org/10.1103/RevModPhys.75.1159>. [arXiv:hep-ph/0212304](https://arxiv.org/abs/hep-ph/0212304)
- B. Grinstein, Y. Grossman, Z. Ligeti, D. Pirjol, Phys. Rev. D **71**, 011504 (2005). <https://doi.org/10.1103/PhysRevD.71.011504>. [arXiv:hep-ph/0412019](https://arxiv.org/abs/hep-ph/0412019)
- D. Becirevic, E. Kou, A. Le Yaouanc, A. Tayduganov, JHEP **1208**, 090 (2012). [https://doi.org/10.1007/JHEP08\(2012\)090](https://doi.org/10.1007/JHEP08(2012)090). [arXiv:1206.1502](https://arxiv.org/abs/1206.1502) [hep-ph]
- F. Bishara, D.J. Robinson, JHEP **1509**, 013 (2015). [https://doi.org/10.1007/JHEP09\(2015\)013](https://doi.org/10.1007/JHEP09(2015)013). [arXiv:1505.00376](https://arxiv.org/abs/1505.00376) [hep-ph]
- E. Kou, A. Le Yaouanc, A. Tayduganov, Phys. Rev. D **83**, 094007 (2011). <https://doi.org/10.1103/PhysRevD.83.094007>. [arXiv:1011.6593](https://arxiv.org/abs/1011.6593) [hep-ph]
- Aaij, Roel et al. [LHCb Collaboration], Phys. Rev. Lett. **112** (2014) 161801. [arXiv:1402.6852](https://arxiv.org/abs/1402.6852) [hep-ex]
- Aaij, Roel et al. [LHCb Collaboration], JHEP **04** (2015) 064. [arXiv:1501.03038](https://arxiv.org/abs/1501.03038) [hep-ex]
- Aaij, Roel et al. [LHCb Collaboration], Phys. Rev. Lett. **118** (2017) 021801. [arXiv:1609.02032](https://arxiv.org/abs/1609.02032) [hep-ex]
- M. Gremm, F. Kruger, L.M. Sehgal, Phys. Lett. B **355**, 579 (1995). [https://doi.org/10.1016/0370-2693\(95\)00722-W](https://doi.org/10.1016/0370-2693(95)00722-W). [arXiv:hep-ph/9505354](https://arxiv.org/abs/hep-ph/9505354)
- T. Mannel, S. Recksiegel, J. Phys. G **24**, 979 (1998). <https://doi.org/10.1088/0954-3899/24/5/006>. [arXiv:hep-ph/9701399](https://arxiv.org/abs/hep-ph/9701399)
- C. S. Huang, H. G. Yan, Phys. Rev. D **59**, 114022 (1999) Erratum: [Phys. Rev. D **61**, 039901 (2000)]. <https://doi.org/10.1103/PhysRevD.59.114022>. <https://doi.org/10.1103/PhysRevD.61.039901>. [arXiv:hep-ph/9811303](https://arxiv.org/abs/hep-ph/9811303)
- G. Hiller, A. Kagan, Phys. Rev. D **65**, 074038 (2002). <https://doi.org/10.1103/PhysRevD.65.074038>. [arXiv:hep-ph/0108074](https://arxiv.org/abs/hep-ph/0108074)
- T.M. Aliev, M. Savci, JHEP **0605**, 001 (2006). <https://doi.org/10.1088/1126-6708/2006/05/001>. [arXiv:hep-ph/0507324](https://arxiv.org/abs/hep-ph/0507324)
- X.G. He, T. Li, X.Q. Li, Y.M. Wang, Phys. Rev. D **74**, 034026 (2006). <https://doi.org/10.1103/PhysRevD.74.034026>. [arXiv:hep-ph/0606025](https://arxiv.org/abs/hep-ph/0606025)
- O. Leitner, Z.J. Ajaltouni, E. Conte (2006). [arXiv:hep-ph/0602043](https://arxiv.org/abs/hep-ph/0602043)
- F. Legger, T. Schietinger, Phys. Lett. B **645**, 204 (2007) Erratum: [Phys. Lett. B **647**, 527 (2007)]. <https://doi.org/10.1016/j.physletb.2006.12.011>. <https://doi.org/10.1016/j.physletb.2007.02.044>. [arXiv:hep-ph/0605245](https://arxiv.org/abs/hep-ph/0605245)
- L. Oliver, J.-C. Raynal, R. Sinha, Phys. Rev. D **82**, 117502 (2010). <https://doi.org/10.1103/PhysRevD.82.117502>. [arXiv:1007.3632](https://arxiv.org/abs/1007.3632) [hep-ph]
- Y.L. Liu, L.F. Gan, M.Q. Huang, Phys. Rev. D **83**, 054007 (2011). <https://doi.org/10.1103/PhysRevD.83.054007>. [arXiv:1103.0081](https://arxiv.org/abs/1103.0081) [hep-ph]
- T. Blake, T. Gershon, G. Hiller, Ann. Rev. Nucl. Part. Sci. **65**, 113 (2015). <https://doi.org/10.1146/annurev-nucl-102014-022231>. [arXiv:1501.03309](https://arxiv.org/abs/1501.03309) [hep-ex]
- E. Leader, E. Predazzi, Camb. Monogr. Part. Phys. Nucl. Phys. Cosmol. **4**, 1 (1996)

28. W.G.D. Dharmaratna, G.R. Goldstein, Phys. Rev. D **53**, 1073 (1996). <https://doi.org/10.1103/PhysRevD.53.1073>
29. M. Galanti, A. Giammanco, Y. Grossman, Y. Kats, E. Stamou, J. Zupan, JHEP **1511**, 067 (2015). [arXiv:1505.02771](https://arxiv.org/abs/1505.02771) [hep-ph]
30. R. Aaij et al. [LHCb Collaboration], Phys. Lett. B **724**, 27 (2013). <https://doi.org/10.1016/j.physletb.2013.05.041>. [arXiv:1302.5578](https://arxiv.org/abs/1302.5578) [hep-ex]
31. CMS Collaboration [CMS Collaboration], CMS-PAS-BPH-15-002
32. H.Y. Cheng, C.Y. Cheung, G.L. Lin, Y.C. Lin, T.M. Yan, H.L. Yu, Phys. Rev. D **51**, 1199 (1995). <https://doi.org/10.1103/PhysRevD.51.1199>
33. H.Y. Cheng, Phys. Rev. D **56**, 2783 (1997). <https://doi.org/10.1103/PhysRevD.56.2783>
34. T. Gutsche, M.A. Ivanov, J.G. Korner, V.E. Lyubovitskij, P. Santorelli, Phys. Rev. D **87**, 074031 (2013). <https://doi.org/10.1103/PhysRevD.87.074031>. [arXiv:1301.3737](https://arxiv.org/abs/1301.3737) [hep-ph]
35. M. Tanabashi et al. [Particle Data Group], Phys. Rev. D **98**, 030001 (2018). <https://doi.org/10.1103/PhysRevD.98.030001>
36. R. Aaij et al. LHCb Collaboration. JHEP **1408**, 143 (2014). [arXiv:1405.6842](https://arxiv.org/abs/1405.6842) [hep-ex]
37. Y.K. Hsiao, P.Y. Lin, L.W. Luo, C.Q. Geng, Phys. Lett. B **751**, 127 (2015). [arXiv:1510.01808](https://arxiv.org/abs/1510.01808) [hep-ph]
38. H.Y. Jiang, F.S. Yu, Eur. Phys. J. C **78**(3), 224 (2018). [arXiv:1802.02948](https://arxiv.org/abs/1802.02948) [hep-ph]
39. R. Aaij et al. LHCb Collaboration. Phys. Rev. D **85**, 032008 (2012). [arXiv:1111.2357](https://arxiv.org/abs/1111.2357) [hep-ex]
40. Y. Amhis et al. [HFLAV Collaboration], Eur. Phys. J. C **77**(12), 895 (2017). <https://doi.org/10.1140/epjc/s10052-017-5058-4>. [arXiv:1612.07233](https://arxiv.org/abs/1612.07233) [hep-ex]
41. R. Aaij et al. LHCb Collaboration. JHEP **1304**, 001 (2013). [arXiv:1301.5286](https://arxiv.org/abs/1301.5286) [hep-ex]
42. R. Aaij et al. [LHCb Collaboration], Phys. Rev. Lett. **118**(5), 052002 (2017). Erratum: [Phys. Rev. Lett. **119**(16), (2017) 169901]. <https://doi.org/10.1103/PhysRevLett.119.169901>. <https://doi.org/10.1103/PhysRevLett.118.052002>. [arXiv:1612.05140](https://arxiv.org/abs/1612.05140) [hep-ex]
43. R. Aaij et al. [LHCb Collaboration], Chin. Phys. C **40**(1), 011001 (2016). <https://doi.org/10.1088/1674-1137/40/1/011001>. [arXiv:1509.00292](https://arxiv.org/abs/1509.00292) [hep-ex]
44. R. Aaij et al., LHCb Collaboration. Phys. Rev. D **99**(5), 052006 (2019). <https://doi.org/10.1103/PhysRevD.99.052006>
45. R. Aaij et al., [LHCb Collaboration] (2019) [arXiv:1902.06794](https://arxiv.org/abs/1902.06794) [hep-ex]
46. M.B. Voloshin (2015). [arXiv:1510.05568](https://arxiv.org/abs/1510.05568) [hep-ph]
47. T. Gleisberg, S. Hoeche, F. Krauss, M. Schonherr, S. Schumann, F. Siegert, J. Winter, JHEP **0902**, 007 (2009). <https://doi.org/10.1088/1126-6708/2009/02/007>. [arXiv:0811.4622](https://arxiv.org/abs/0811.4622) [hep-ph]
48. M. Bahr et al., Eur. Phys. J. C **58**, 639 (2008). <https://doi.org/10.1140/epjc/s10052-008-0798-9>. [arXiv:0803.0883](https://arxiv.org/abs/0803.0883) [hep-ph]
49. T. Sjostrand, S. Mrenna, P.Z. Skands, Comput. Phys. Commun. **178**, 852 (2008). <https://doi.org/10.1016/j.cpc.2008.01.036>. [arXiv:0710.3820](https://arxiv.org/abs/0710.3820) [hep-ph]
50. Y.M. Wang, Y. Li, C.D. Lu, Eur. Phys. J. C **59**, 861 (2009). <https://doi.org/10.1140/epjc/s10052-008-0846-5>. [arXiv:0804.0648](https://arxiv.org/abs/0804.0648) [hep-ph]
51. R. Aaij et al., LHCb Collaboration. Phys. Rev. Lett. **123**(3), 031801 (2019). <https://doi.org/10.1103/PhysRevLett.123.031801>
52. A. Davies et al., *PatLongLivedTracking: a tracking algorithm for the reconstruction of the daughters of long-lived particles in LHCb*; LHCb-PUB-2017-001; CERN-LHCb-PUB-2017-001. <https://cds.cern.ch/record/2240723>
53. A.M. Sirunyan et al. [CMS Collaboration], Phys. Rev. D **97**(7), 072010 (2018). <https://doi.org/10.1103/PhysRevD.97.072010>
54. R. Aaij et al. [LHCb Collaboration], Int. J. Mod. Phys. A **30**(07), 1530022 (2015). <https://doi.org/10.1142/S0217751X15300227>. [arXiv:1412.6352](https://arxiv.org/abs/1412.6352) [hep-ex]
55. A.A. Alves Jr. et al. LHCb Collaboration. JINST **3**, S08005 (2008). <https://doi.org/10.1088/1748-0221/3/08/S08005>
56. A. Roel et al. [LHCb Collaboration], JHEP **09**, 146 (2018). [arXiv:1808.00264](https://arxiv.org/abs/1808.00264) [hep-ex]
57. I. Bediaga et al. [LHCb Collaboration], *LHCb Tracker Upgrade Technical Design Report*; CERN-LHCC-2014-001; LHCb-TDR-015 (2014)
58. A.A. Alves Jr. et al. [LHCb Collaboration], *LHCb Trigger and Online Upgrade Technical Design Report*; CERN-LHCC-2014-016; LHCb-TDR-016 (2014)
59. A. Paul, D.M. Straub, JHEP **1704**, 027 (2017). [https://doi.org/10.1007/JHEP04\(2017\)027](https://doi.org/10.1007/JHEP04(2017)027)
60. D.M. Straub, [arXiv:1810.08132](https://arxiv.org/abs/1810.08132) [hep-ph]